Atmospheric Stratification and Radiative Transfer

Y. Grosdidier,S. Lovejoy
McGill University
Montreal, Canada

B. P. Watson
St. Lawrence University
Canton, New York

D. Schertzer
École Nationale des Ponts et Chaussées
Toulouse, France

Introduction: Differential stratification and convection of the atmosphere over wide ranges of scales

Theories of atmospheric dynamics, turbulence, cloud structure and atmospheric radiative transfer are nearly all based on the idea that at small enough scales, structures are three dimensional whereas, at large scales they are two dimensional. Clouds can readily be hundreds or thousands of kilometers long, however due to gravity, they form layers which are not nearly so thick: when viewed from space the entire atmosphere appears as an envelope roughly 10 km thick surrounding the Earth like an onion skin. This has lead to the popular idea that the large scale structures - the "weather" - is more nearly two dimensional; theoretically it is justified by the "quasi-geostrophic" approximation.

When we say that clouds or other atmospheric structures are "3-D like", we mean that on average they are the same in all directions so that a cloud 10 times larger will fill up a volume of space 103 = 1000 times bigger. On the other hand, the large scale clouds would have roughly constant thickness so that the volumes of 10 times larger clouds would be 102 = 100 times bigger. According to this, at human scales, clouds and other structures are 3-D like but undergo a qualitative transition to large scale 2-D like behavior. Since the 1960's, this has been the dominant model of the atmosphere (Monin 1972. Pedlosky 1979).

Meteorologists exploit the supposedly 2-D like nature of the large scale weather to filter out the small scale supposedly 3-D turbulence which is thus reduced to a kind of background noise. But what is the dimension of the atmosphere? In a 2-D atmosphere there is only variability in the horizontal direction; in a 3-D atmosphere, the variability is isotropic: on average, if we go a distance Δx in the horizontal, we must go a distance $\Delta z = \Delta x$ in the vertical to obtain the same variation in the field. In an intermediate stratified but still scaling case, we must go only a distance $\Delta z = \Delta x^{H_z}$, with $0 < H_z < 1$ so that $H_z = 1$ corresponds to 3-D isotropy, $H_z = 0$ to 2-D (isotropy in the horizontal plane). The size of typical

structures thus varies as $\Delta x \Delta x \Delta x^{Hz} = \Delta x^{D}$ with $D = 2+H_z$. The intermediate dimension D is called an "elliptical dimension" because of the typical elliptical shapes of the vertical section of the average structures.

Twenty years ago (Schertzer and Lovejoy 1983, Schertzer and Lovejoy 1985a, Schertzer and Lovejoy 1985b) proposed that horizontal structures were dominated by energy fluxes, while the vertical ones were dominated by buoyancy variance fluxes so that Hz = 5/9, D = 23/9 ≈ 2.555. The difficulty was that until now, tests were made using either aircraft wind data in the horizontal or balloon wind data in the vertical. The results from separate experiments (with the partial exception of Chigirinskaya et al. 1994, and Lazarev et al. 1994) often from different parts of the world and under different conditions, could only be compared in an indirect way. An additional problem is that aircraft do not fly in perfectly flat trajectories nor do balloons rise in perfect vertical paths. Indeed, it has only recently been discovered (Lovejoy et al. 2004) that due to non 2-D turbulence, aircraft can follow fractal trajectories. Therefore, aircraft data can yield spurious statistical exponents leading to incorrect interpretations. Finally, huge amounts of data are needed in order to average over the large fluctuations to get accurate results.

A new study (Lilley et al. 2004) based on 9 airborne lidar vertical cross-sections of pollution and covering the range 3 m to 4,500 m in the vertical, and 100 m to 120 km in the horizontal finally seems to provide fairly conclusive evidence for the 23/9-D model: it yielded D = 2.55±0.02, so that the 2-D and 3-D theories are well outside the one standard deviation error bars (see Figure 1). These error bars are particularly small since each of the 9 sections has nearly 100 times the amount of data of the largest comparable balloon experiment (involving 280 ascents). The pollution acts as a tracer, reflecting light back to a telescope in the aircraft, allowing us to directly deduce the degree of stratification of the structures as functions of their horizontal extents. The horizontal range is particularly significant since it spans that critical 10 km scale where the 3-D to 2-D transition ought to occur. In addition each data set was obtained within a short period of time (about 20 minutes) so that the meteorology was roughly constant. The result D = 2.55±0.02 is almost exactly that predicted from the 23/9 dimensional model and shows that even at scales as small as 3 m the atmosphere does not appear to be three dimensional, nor at large scales does it ever appear to be perfectly flat, two dimensional, rather structures simply become more and more (relatively) flat as they get larger and larger.

A major consequence is that differential stratification allows us to understand the horizontal statistics of clouds. (Lovejoy et al. 2001) showed by analysis of nearly 1000 satellite pictures that the (multi)scaling is obeyed to within 1.5% /octave in scale over the range 5000 km down to 1 km, and that the radiances (IR and visible wavelengths) are (to within roughly this error) those that would occur if the radiances were the outcome of cascade processes starting at near 20,000 km, i.e. planetary sizes. (Sachs et al. 2002) extended these analyses down to below 1 m in scale.

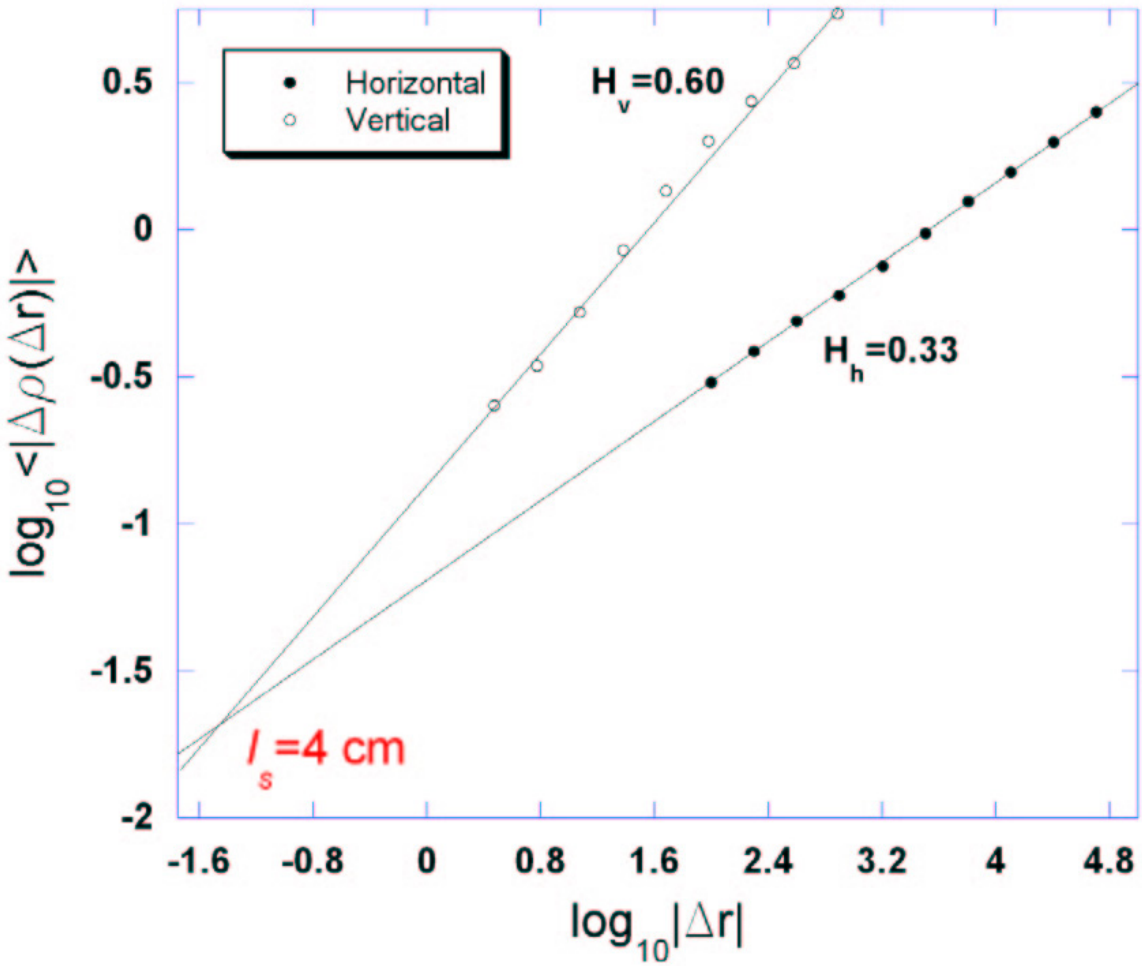

Figure 1.. The first order structure functions for the fluctuations in lidar aerosol backscatter ratio (passive scale surrogate) as a function of horizontal wave-number; top vertical direction, bottom, horizontal direction.. The curves are the average of 9 airborne lidar transects over the range 3 m to 3 km, and from 96 m to 80 km in the horizontal. The lines have purely theoretical slopes (Hh = 1/3, Hv = 3/5), only the offsets are determined by regression. The intersection point (4 cm) is the scale at which typical vertical and horizontal fluctuations are equal in magnitude. At this scale, structures are roundish, hence the name "sphero-scale". This is determined by the local buoyancy force variance flux and energy fluxes.

Some implications for radiances and models

In the atmosphere, significant nonlinear interactions occur over ranges in space of about millimeters to thousands of kilometers, and in time from at least milliseconds to thousands of years. However, General Circulation Models (GCM) are limited to roughly two orders of magnitude in (horizontal) space (20,000 km / 200 km), four orders of magnitude in time (century / day) and one order of magnitude in the vertical. This obvious limitation of range of scales leads to the consideration of single column models (SCM) (Iacobellis and Somerville 1991a, Iacobellis and Somerville 1991b)] as alternatives/complements

to GCMs. SCMs have much wider vertical ranges (by factors of 100 – 1,000), but have only a single pixel in the horizontal.

From the point of view of realistic treatment of radiative effects, these models have two related weaknesses. First, the SCM is purely 1-D and the GCM has relatively few vertical levels. SCMs do not properly represent the cloud structures which are expected to be 2.55-D. In contrast, a GCM with a factor 100 in horizontal resolution and 1000.5 in the vertical corresponds to a 2.5-D model, however with severe truncation in scale. To gage the significance of this for radiances, see Figures 2a and 2b which show that the visible and IR radiance variabilities build up scale by scale so that the second statistical moment increases roughly by a factor of 2 every factor of 100 in scale (cf. the top curves which are for the q = 1.6 order moments).

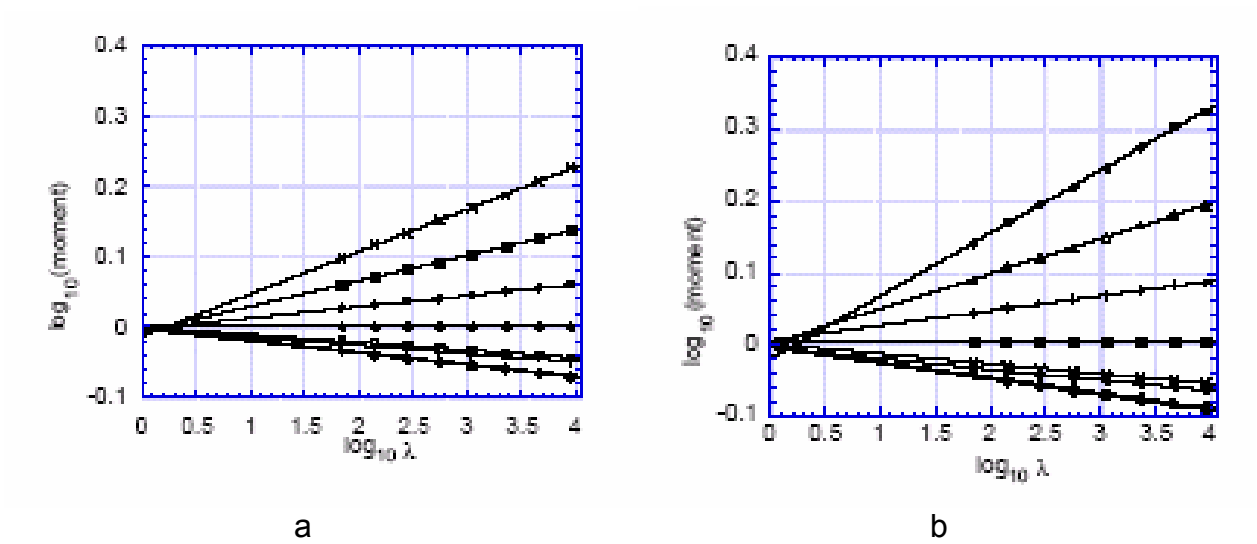

Figure 2.. a. Isotropic statistical moments of order 0.2, 0.4, 0.6, 0.8, 1, 1.2, 1.4 and 1.6 as a function of spatial resolution for the absolute gradients of 161 NOAA14 visible images (roughly every 2 days for a year) over the Oklahoma ARM CART site (Lovejoy et al. 2001). λ = L/L0 with L0 = 20,000 km..
b. Same but for 353 (roughly every day for a year) NOAA14 IR images over the Oklahoma ARM CART site (Lovejoy et al. 2001). Different cloud types/morphologies lead to anisotropic scaling which is effectively "washed out" by the angle averaging in the above statistics.

According to Lovejoy et al. (2001) and Sachs et al. (2002), this continues over the range 104 km to 1 m (a range of 107). In comparison, the GCM can only estimate the fluctuations on a much larger artificial inner scale, instead of the natural one, so that there is much less variability. The loss of variability due to this factor of 105 reduction in range of scales can be directly estimated from Figures 2a and 2b for the moments up to order 1.6; for the (not shown) second order moment we find a reduction by a factor of 6. However, the extremes are much more affected: for example, at visible wavelengths, we obtain a factor of nearly 105 for the 4th order moment.

A direct implication of these extreme, nonclassical statistics is that they imply a strong resolution dependence of meteorological quantities. Of particular relevance for this project is the fact that cloud fraction – like the length of coastlines – fundamentally depends on the resolution at which it is measured (Gabriel et al. 1988, Lovejoy and Schertzer 1990, Tessier et al. 1993, Davis et al. 1996, Davis et al. 1997).

Key ARM objectives include the understanding and modeling of 3-D cloud-radiation processes for both water and aerosol clouds. Over huge ranges of space-time scales, the corresponding dynamical cloud processes are highly variable and turbulent. If the atmosphere is not 2-D, then there are at least two important consequences for the transfer: i) the first (Schertzer et al. 1997a) is that tubes of radiative fluxes (at least in optically thick clouds) will be fractal so that a fractal extension of the classical Independent Pixel Approximation (IPA) must be made. Since fractal tubes are much longer than non-fractal ones, the intensity/optical thickness relations are expected to be quite different; ii) the second consequence is that the tubes will be anisotropic fractals with exponents dependent on the elliptical dimension D.

By using cascade based scaling stratified cloud models (SSCMs) and various radiative transport techniques (especially sparse matrix inversion and discrete angle phase function for the optically thick clouds) (Lovejoy et al. 1990, Gabriel et al. 1990, Davis et al. 1990), we can directly investigate the effects of stratification. By explicitly and realistically modeling the stratification we therefore aim to provide the key link between the horizontal radiance fields, the cloud liquid water and aerosol concentration fields. Figure3 gives an example of a multifractal model of cloud liquid water density showing the potential for simulating radiation at different wavelengths. In the next sections we give more details and examples.

The multifractal models

A convenient way to discuss the scaling properties of a multifractal field (such as the liquid water density field in the following) is to consider the following multiscaling statistics:

$$\begin{aligned} \Delta\rho(\underline{\Delta X}) &= \rho(\underline{\Delta X} + \underline{X}) - \rho(\underline{X}) \\ \left\langle \left| \Delta\rho\left(\lambda^{-1}\underline{\Delta X}\right) \right|^q \right\rangle &= \lambda^{-\xi(q)} \left\langle \left| \Delta\rho(\underline{\Delta X}) \right|^q \right\rangle \end{aligned} \tag{1}$$

where $\xi(q)$ is the scaling moment function. In the above, X=(x,y,z,t), i.e. we consider at the outset a space-time scaling process. This equation relates fluctuations at large scales and scales reduced by factor λ.

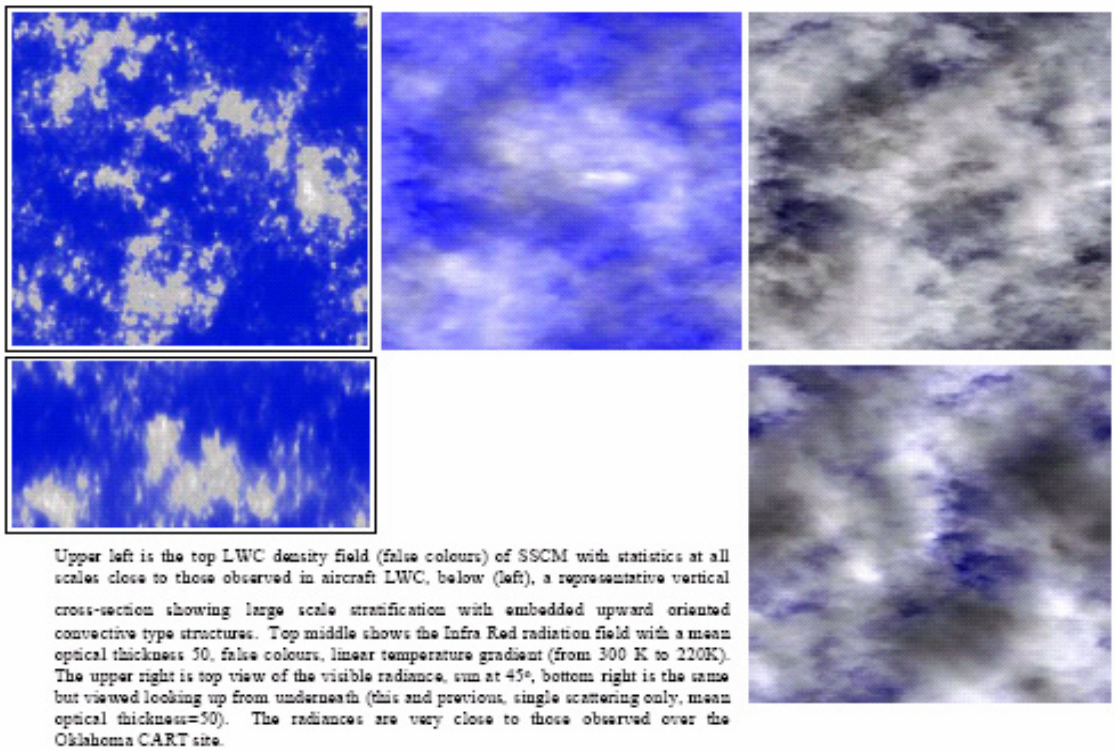

Figure 3.. An illustration of a scaling stratified 3-D cloud model (SSCM) on a 128 x 256 x 256 grid (single scattering only). The differential stratification parameters are Hz = 5/9 (cf. Figure 1), sphero-scale = 1 pixel. Also the statistical parameters are α=1.8, C1=0.1, H=1/3 (close to those obtained from analysis of Figure 1 visible radiances; see also section 3.).

In the last 20 years, in geophysics alone (for reviews – Lovejoy and Schertzer 1991, Lovejoy and Schertzer 1995, Schertzer et al. 1997b) there have been over twenty different fields where multifractal behavior has been found. In some cases – notably the topography and cloud radiances – particularly wide ranges have been empirically demonstrated (planetary scales down to <40 m and planetary scales down to <1 m respectively (Gagnon et al. 2004, Lovejoy et al. 2001, Sachs et al. 2002). The generic multifractal process is cascades; these occur in systems with large number of degrees of freedom where the same basic dynamical mechanism operates over a wide range of scales (i.e. when it is scale invariant in some very general sense; see also *Anisotropic scaling*), and in which some flux is conserved from one scale to another, the interactions being mostly between structures at neighboring scales.

In spite of its importance, there has been surprisingly little attention paid to the numerical modelling of realistic multifractal clouds. With only a few exceptions, simulations in the literature are discrete in scale, (almost invariably with cascades step ratio = 2), which yield visually weird (unrealistic straight line structures), highly artificial simulations. Other limitations of the standard "toy" cascades include isotropy (self-similarity), left-right symmetry (which precludes causal processes) and conservation (with scale) of the mean.

Anisotropic scaling

Figures 2a and 2b show that the isotropic statistics of visible and infrared radiances are very close to those indicated in Equation 1. This implies that the differences between different clouds with different morphologies is in their anisotropic scaling characteristics.

In order to consider anisotropic processes, we replace the isotropic reduction $\underline{\Delta X} \rightarrow T_\lambda \underline{\Delta X}$ by the more general anisotropic reduction $\underline{\Delta X} \rightarrow \lambda^{-1} \underline{\Delta X}$ where T_λ is a scale changing operator. This, combined with a definition of the unit "ball" (upon whose boundary lie all the unit vectors) defines the scale (λ) of all the vectors. Often, the unit ball is a sphere, i.e. the corresponding "sphero-scale" (denoted ls) is isotropic.. Since the system is scale invariant, T_λ must have group properties; in particular it is defined by an operator called a "generator" G:

$$T_\lambda = \lambda^{-G} \tag{2}$$

T□ is a generalized "zoom" by factor λ. When G is a matrix, then we have linear Generalized Scale Invariance (GSI) (Schertzer and Lovejoy 1985b), the notion of scale being independent of location. Within linear GSI, we recover the familiar case of self-similarity when G is the identity matrix. However, when G is diagonal, we recover self-affinity. With off-diagonal elements, structures are stratified with finite rotation with scale (real eigenvalues), or with unlimited rotation (complex eigenvalues). The minimum needed to model clouds with horizontal texture (c, f, e parameters), advection (Ax, Ay parameters), vertical and temporal stratification (Hz, Ht) is:

$$G = \begin{pmatrix} 1+c & f-e & 0 & A_x \\ f+e & 1-c & 0 & A_y \\ 0 & 0 & H_z & 0 \\ 0 & 0 & 0 & H_t \end{pmatrix} \tag{3}$$

for vectors X=(x,y,z,t) where for the wind, dimensional analysis and empirical measurements give Hz = 5/9 (Schertzer and Lovejoy 1985b), Ht = 2/3 (Lovejoy and Schertzer 1990) (this is sometimes called the "dynamical scaling exponent"). The values of c, f and e control the differential rotation, stratification, "texture". The 2x2 upper left submatrix controls the horizontal structure, the eigenvalues are d ± a with a2 = c2 + f2 - e2. When a2 > 0, there is stratification dominance, when a2<0, rotation dominance.. Different cloud/rain morphologies involve specific types of spatially varying textures, the above linear generator is simply a linear approximation to a more general nonlinear generator. As indicated in (Schertzer et al. 1997b), as required by the underlying physics, the above satisfies Galilean invariance, Ax and Ay are linear functions of the advection velocity.

Finally, we can decompose the function ξ(q) (see *The Multifractal models*) into two parts:

$$\xi(q) = qH - K(q) \tag{4}$$

where H is a "Hurst exponent" (although not the one originally introduced by Hurst!) and K(q) represents the contribution of a cascade process: it is nonlinear with K(1)=0. When K(q)=0, ξ (q)=qH and the process is a variety of simple scaling (e.g fractional Brownian motion "fBm" (Mandelbrot and Van Ness 1968), or fractional Lévy motion if ξ (q = α) diverges for a critical $\alpha < 2$). The only general constraint on K(q) is that it is a convex function – in general it requires an infinite number of theoretical or empirical parameters. Hence that without further assumptions modeling and analysis would be impossible. This is the problem of "universality".. In the case of multifractals, due to the nontrivial, singular small scale limit, the question of universality was long confused. It is now clear that "universal multifractals" do exist [see the debate – Schertzer and Lovejoy 1997, Gupta and Waymire 1997).

Universal multifractals (Schertzer and Lovejoy 1987, Schertzer et al. 1997b), which are often misnamed "Log-Levy", are the multiplicative analogues of the (additive) central limit theorem, with the following moment scaling function:

$$K(q) = \frac{C_1}{\alpha - 1}\left(q^{\alpha} - q\right) \tag{5}$$

where C1 is the codimension of the mean, and α is the Lévy index of the generator. Note that due to the singular small scale limit, Equation 5 will generally only hold up to a critical upper limit q_D after which the moments will diverge (leading to algebraic, "fat tails"). Note that Log-Poisson processes have been lately in vogue (She and Levesque 1994). However, they are only "weakly" universal in the sense that while their generators do allow the process to be continuous in scale, they are not stable or attractive. In addition, the Log-Poisson model is nothing more than a continuous in scale limit (Schertzer et al. 1995) of the pedagogical but simplistic α model (Schertzer and Lovejoy 1983) sharing most of its limitations. Furthermore, the usual choice of parameters for the Log-Poisson model is incompatible with the commonly observed power law tails on probability distributions..

Unit ball, differential stratification

To illustrate these ideas, consider Figure 4 which shows the single scattered radiation field of a multifractal cloud with the observed isotropic statistics (α, C1, H) as well as the observed differential stratification between the horizontal and vertical (Hz = 5/9). The differences are only in the definition of the unit ball, yet there can be substantial differences in the morphologies. Figures 5a, b, c on the contrary show examples with identical unit balls (spherical at a one pixel scale) but with different Hz, i.e. with different differential stratifications: looking at the side views, we see that larger structures become progressively flatter at larger and larger scales with Hz = 5/9 (left); in the center column (Hz = 1), structures stay roughly the same as functions of scale whereas at right (with Hz = 3/2), structures become more vertically stratified at larger and larger scales.

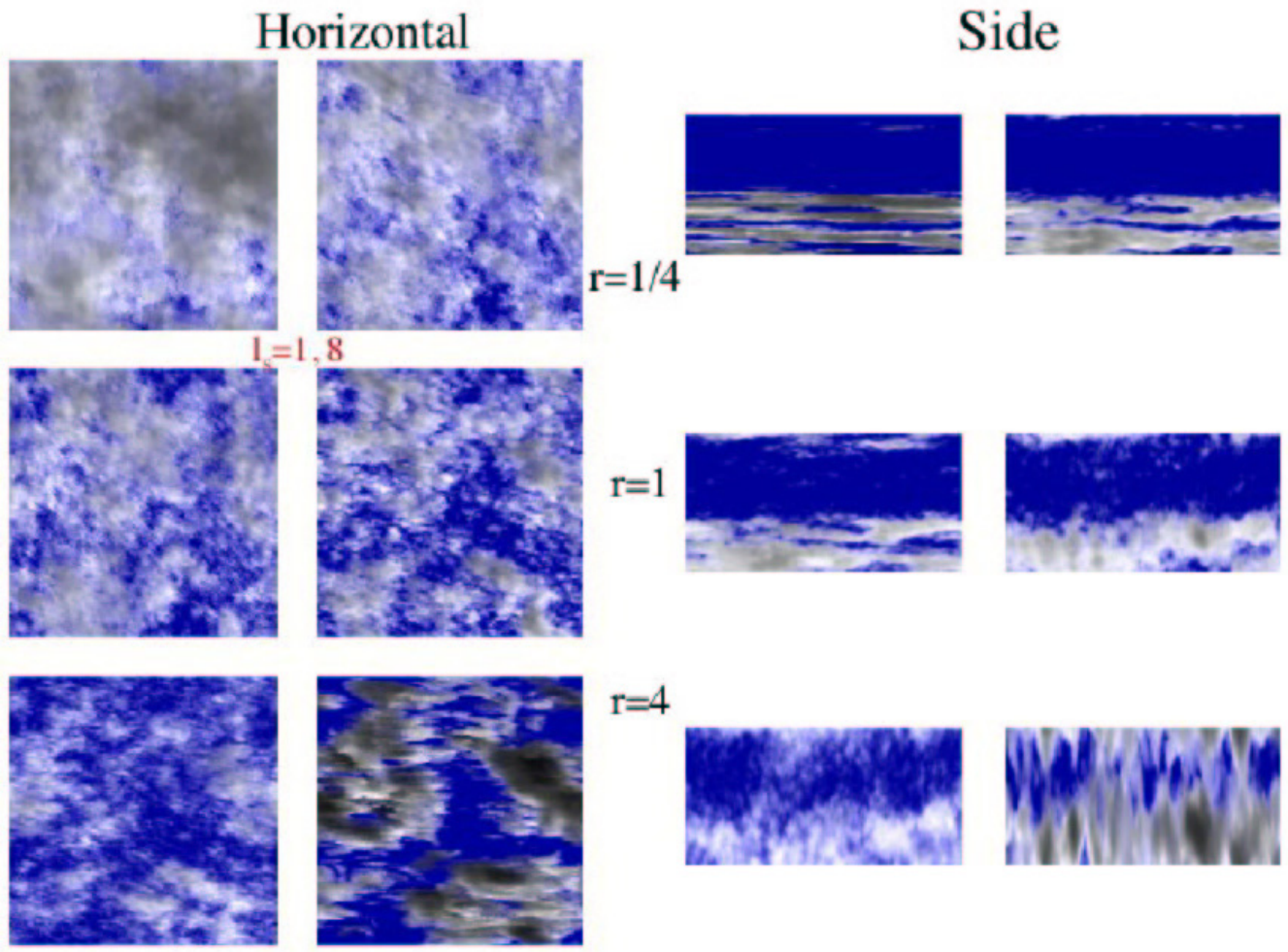

Figure 4.. Left two columns show the horizontal radiance field (single scattering only) of the same basic cloud (generated by the same random seed) but with different sphero-scales (left column ls = 1 pixel, right column, ls = 8 pixels). As we move from top to bottom, the horizontal/vertical aspect ratio (r) at the sphero-scale is varied as indicated. The basic statistics (□, C1, H) are close to those estimated empirically (□=1.8, C1=0.1, H=1/3).. In the right two columns we can see the effect on the structures more clearly. Although the horizontal fields have isotropic statistics at all scales very close to those of real clouds, the morphologies are quite different. In the horizontal these clouds are rotation dominant, but with small differential anisotropy (d = 1, c = 0.1, e = 0.2, f = 0).

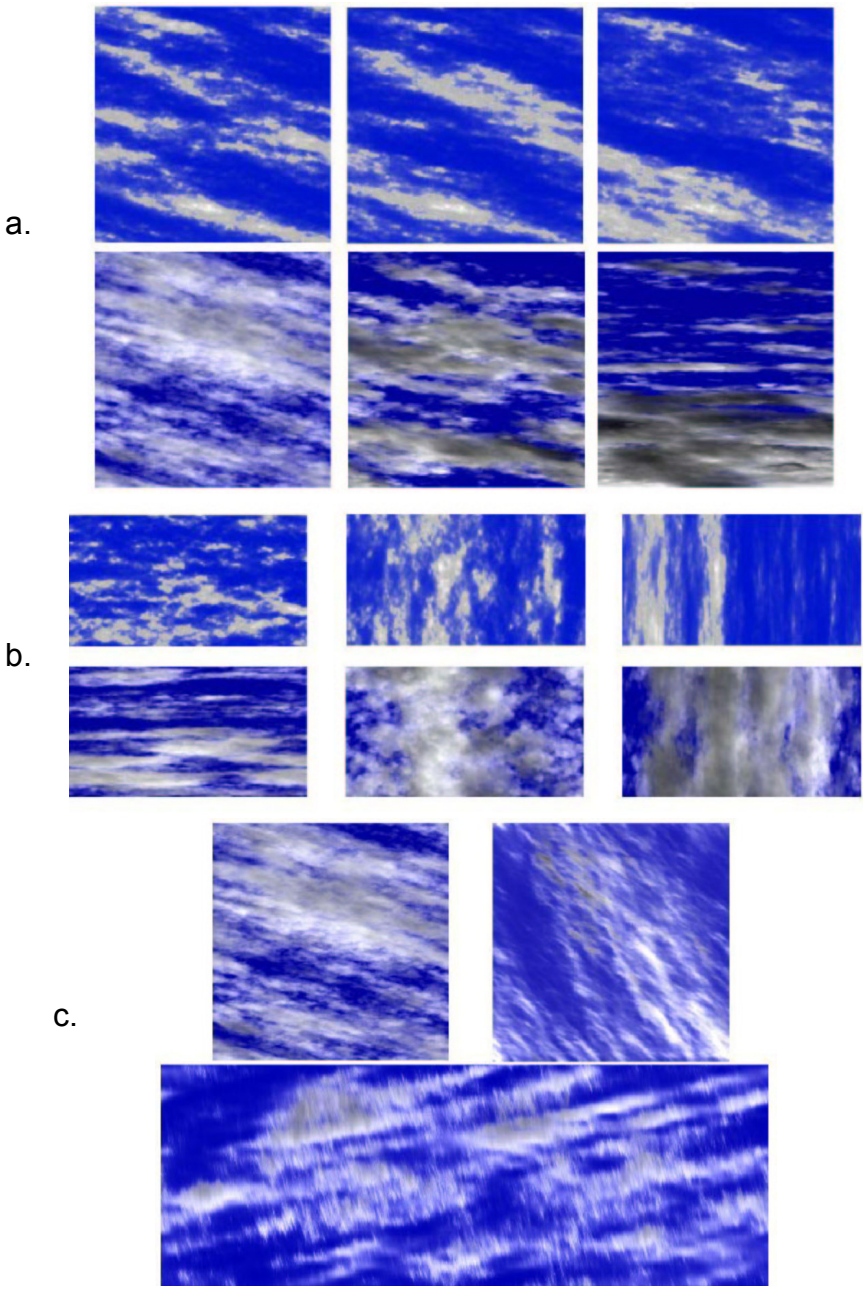

Figure 5.. a.. In these examples, the same basic cloud is shown with the same unit ball (a sphere at a one pixel scale), but with different differential anisotropies (Hz = 5/9, left column, Hz = 1, middle, Hz = 3/2, right). The horizontal anisotropy is characterized by d=1, c=0.2, e=0.1 and f=0. The top row is the liquid water density (false colors), the bottom row shows the single scattered radiation fields (Sun at 45o). The mean optical thickness was taken as 20.. b.. Same but for side views. This clearly shows the effect of changing the differential anisotropy.. From Figure 5a we see that it (more subtly) affects the radiation fields.. c.. These figures again have the observed horizontal isotropic statistics and observed vertical stratification (Hz = 5/9); the only differences are in the unit balls and the horizontal scaling exponents. By having strong stratification (e.g. c=0.4, f=0.1) with a little rotation (e=0.1), we can simulate cirrus clouds (mean optical thickness=1).

Multiple Scattering

The above simulations illustrated the various possibilities of calculating radiative transfer on 3-D multifractal clouds with realistic stratification and horizontal anisotropies. In order to rapidly and highly accurately calculate the multiply scattered radiation, the Discrete Angle Radiative Transfer (DART) method (Lovejoy et al. 1990) is used. The idea is to use rather special phase functions composed of Dirac delta functions at orthogonal angles. (Lovejoy et al. 1990) have shown that in optically thick clouds the scaling exponents do not depend on the phase functions (the prefactors however do depend on them), hence DART allows us to determine the general scaling properties of the radiation fields. The simplest 2-D (3-D) DART approach allows interactions among squares (cubes) only in the one direction perpendicular to each of the 4 (6) faces of a square (cube) (see Figure 6, Top, for the 2-D case). The steady-state radiative transfer equation is then replaced by a linear algebra problem involving a finite scattering matrix (the phase function is now a sum of 4 (6) Dirac functions).

Using new highly accurate, rapid sparse matrix methods, one is therefore in a position to solve exactly and rapidly the radiative transfer equation in a great variety of non homogeneous media including multifractal stratified clouds.. Figure 7 shows a vertical cross-section of stratified cloud and the corresponding horizontal and vertical fluxes when a Gaussian light source is used. See also Figure 8 which shows the same cloud but with a uniform light source from above and where the flux lines have been added.

These simulations promise to allow us to understand the statistical relation (at all scales) between the radiative fluxes and the liquid water density. For example, Figure 9 shows a preliminary result indicating the relatively simple relations between the 1-D energy of the cloud and radiative flux components.. The flat spectra indicate that the vertical (z) flux in the horizontal direction (x) and the horizontal flux in the horizontal direction have nearly identical statistics to the density field in the horizontal; however the fluxes in the vertical directions are different (cf. reference lines with slopes –1, -3/2). There appears to be a range of scales of about 25 necessary for convergence to the low frequency scaling behavior..

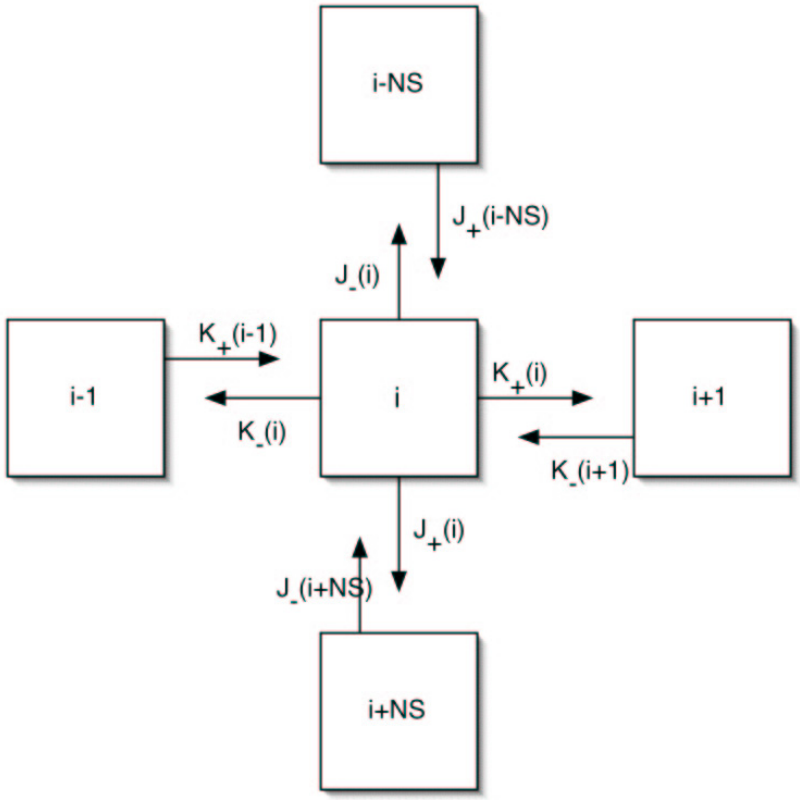

$$J_+(i) = t(i)\, J_+(i - \mathrm{ns}) + r(i)\, J_-(i + \mathrm{ns}) + s(i)\, (K_+(i-1) + K_-(i+1))$$
$$J_-(i) = t(i)\, J_-(i + \mathrm{ns}) + r(i)\, J_+(i - \mathrm{ns}) + s(i)\, (K_+(i-1) + K_-(i+1))$$
$$K_+(i) = t(i)\, K_+(i-1) + r(i)\, K_-(i+1) + s(i)\, (J_+(i - \mathrm{ns}) + J_-(i + \mathrm{ns}))$$
$$K_-(i) = t(i)\, K_-(i+1) + r(i)\, K_+(i-1) + s(i)\, (J_+(i - \mathrm{ns}) + J_-(i + \mathrm{ns}))$$

$$\left(\begin{pmatrix} m_{11} & m_{12} & m_{13} & m_{14} \\ m_{21} & m_{22} & m_{23} & m_{24} \\ m_{31} & m_{32} & m_{33} & m_{34} \\ m_{41} & m_{42} & m_{43} & m_{44} \end{pmatrix} - e\right) \begin{pmatrix} J_+ \\ J_- \\ K_+ \\ K_- \end{pmatrix} = -\begin{pmatrix} S \\ 0 \\ 0 \\ 0 \end{pmatrix}$$

Figure 6.. A schematic diagram showing discrete angle radiative transfer in 2-D discretized onto a rectangular grid for the intensities J+, J-, K+, K- at a given grid point (Top), and in sparse matrix form (Middle and Bottom equations, S is the source function)..

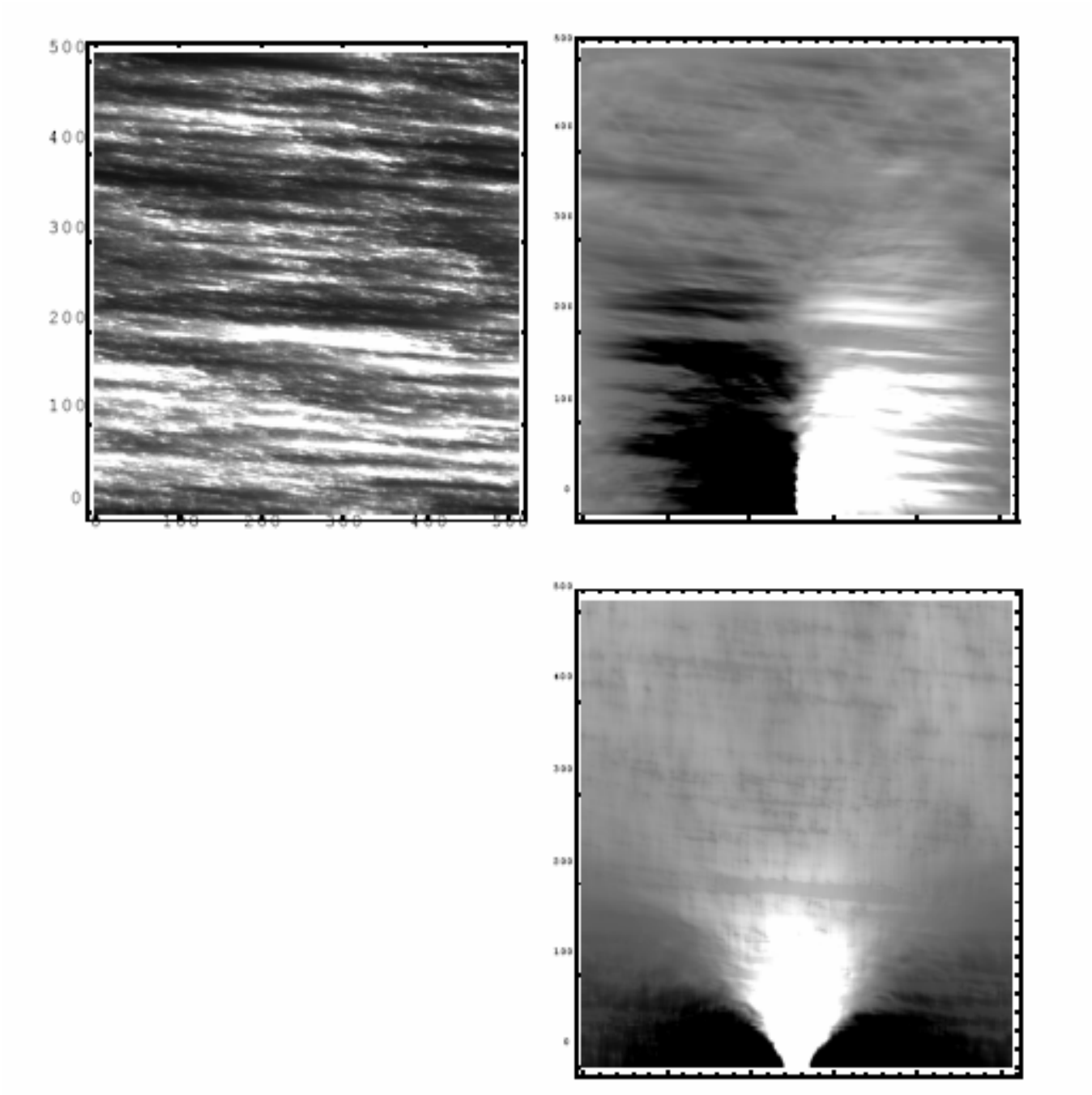

Figure 7.. An example of the Discrete Angle Radiative Transfer (DART) method ([Lovejoy et al., 1990]) on a 512x512 grid. Top left image: LWC of a 2-D horizontally stratified multifractal field (Hz = 5/9) with mean optical thickness 128. Top right image: horizontal radiance fluxes (conservative and isotropic scattering) for a Gaussian source beam of width 10 pixels impinging the cloud at the bottom. Bottom right image: same but for the vertical fluxes. On a Macintosh computer it takes about 30 s to invert the 220x220 sparse matrices needed to solve for the transfer.

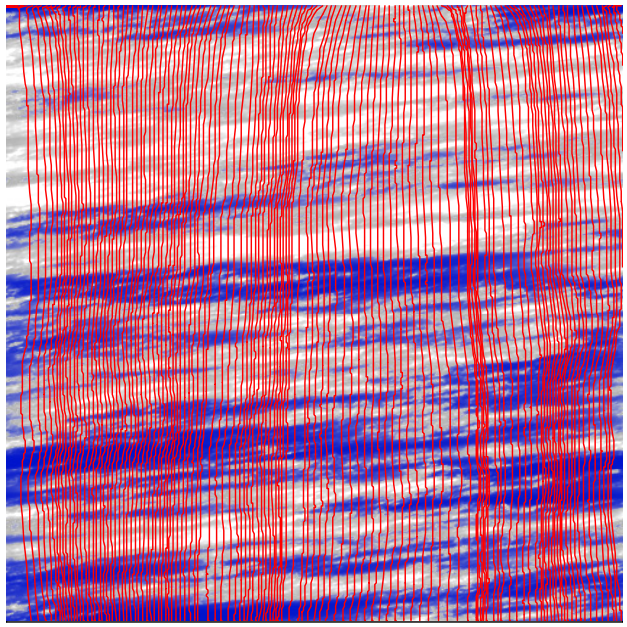

Flux lines (input from top); multifractal IPA

Figure 8.. This figure shows the same cloud (see Figure 7) but with a uniform light source from above; the flux lines have been added. According to the multifractal generalization of the Independent Pixel Approximation [IPA; (Schertzer et al., 1997a)], the IPA should apply but to these (now fractal) flux tubes.. Mean optical thickness=256.

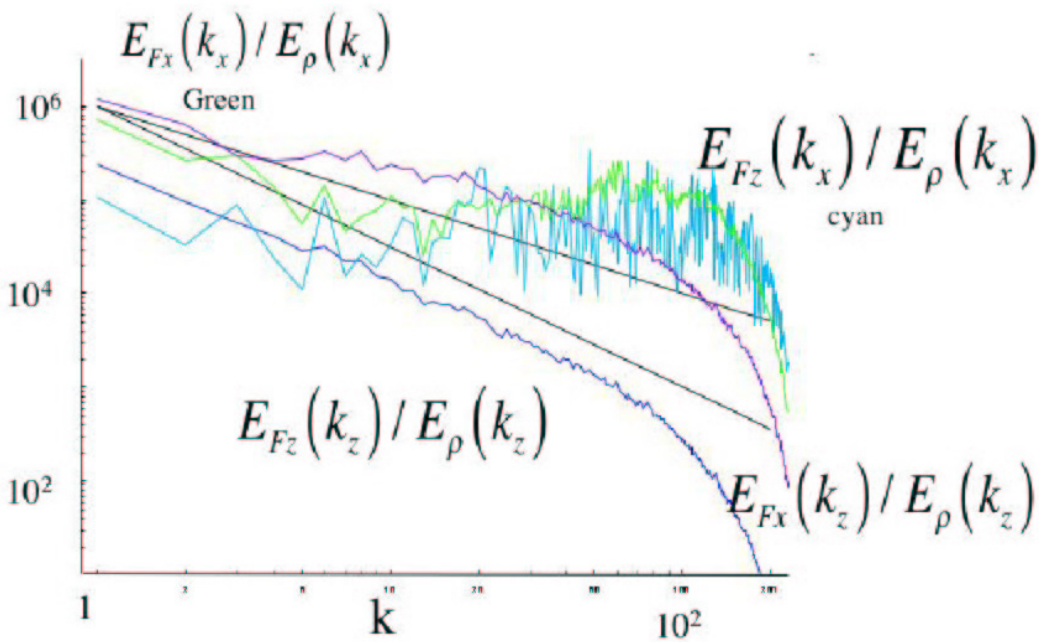

Figure 9.. A comparison of the fluxes of the cloud in Figure 8. Mean optical thickness=256.

Conclusions

The primary strength of the GCMs is that they explicitly account for many of the complex non-linear dynamical interactions. The GCMs have been developed in conjunction with SCMs which allow more complex interactions to be studied at a higher vertical resolution. In contrast, the great strength of the multifractal models is that they inherently take into account interactions over arbitrary ranges of scales. A key goal of our work is to develop Scaling Stratified Cloud Models (SSCMs) that are already available with an adequate degree of scaling stratification, to parameterise clouds in SCMs or GCMs. A SSCM could be regarded as filling the gap between the totally convective SCM and the overly (scale) truncated GCM (see Figures 2a and 2b for an example with convection occurring within an horizontally stratified layer).

A satisfactory GCM cloud modelling scheme is still unavailable due to the fundamental fact - emphasized by (Ricard and Royer 1993) - that clouds can definitively not be considered as clusters of very small droplets floating in the air: they are associated with latent heat release and with turbulent motions that perform major vertical redistributions of sensible heat, moisture and momentum.

Radiation, latent heat and turbulence are the three strongly interacting cloud processes which occur on a wide range of scales and are of fundamental importance for the cloud climate problem. Classical parameterisations are not directly based on interactions between these three processes. Indeed, they are based on rather ad-hoc distributions of a random variable (not a field) representing the sub-grid moisture. This distribution is usually described by its first statistical moments, e.g. a (non skewed) Gaussian distribution (Sommeria and Deardorff 1977), a (skewed) gamma distribution (Bougeault 1982), a (skewed) exponential distribution (Ricard and Royer 1993). This distribution is used to estimate the fraction of the grid that is saturated, hence cloudy, and its liquid water content. Furthermore, the sub-grid heterogeneity is considered to be 2-D, i.e. only on the horizontal: the fraction of clouds inside of the grid box are vertical cylinders. As a very unfortunate consequence, the overall radiative treatment requires further hypotheses on the vertical connection between different layers. This short summary points out the crucial need to greatly improve the cloud parameterisation schemes in order to much better take into account the variability of clouds at a given, as well as over a wider range of scales.

References

Bougeault, P., 1982: Cloud-ensemble relations based on the gamma probability distribution for the higher-order models of the planetary boundary layer, *J. Atmos. Sci.*, **39**, 2691-2700.

Chigirinskaya, Y., D. Schertzer, S. Lovejoy, A. Lazarev, and A. Ordanovich, 1994: Unified multifractal atmospheric dynamics tested in the tropics Part 1: horizontal scaling and self organized criticality, *Nonlinear Processes in Geophysics*, **1**, 105-114.

Davis, A., S. Lovejoy, P. Gabriel, D. Schertzer, and G.L. Austin, 1990: Discrete Angle Radiative Transfer. Part III: Numerical results on homogeneous and fractal clouds, *J. Geophys. Res.*, **95**, 11729-11742.

Davis, A., A. Marshak, W. Wiscombe, and R. Cahalan, 1996: Scale Invariance of liquid water distributions in Marine Stratocumulus. Part I: Spectral properties and stationarity issues., *J. Atmos. Sci.*, 53, 1538-1558.

Davis, A., A. Marshak, W. Wiscombe, and R. Cahalan, 1997: Scale Invariance of liquid water distributions in Marine Stratocumulus. Part II: Multifractal properties and intermittency issues, *J. Atmos. Sci.*, **54**, 1423-1444.

Gabriel, P., S. Lovejoy, D. Schertzer, and G.L. Austin, 1988: Multifractal Analysis of resolution dependence in satellite imagery, *Geophys. Res. Lett.*, **15**, 1373-1376.

Gabriel, P., S. Lovejoy, A. Davis, D. Schertzer, and G.L. Austin, 1990: Discrete Angle Radiative Transfer. Part II: renormalization approach to scaling clouds, *J. Geophys. Res.*, **95**, 11717-11728, 1990.

Gagnon, J.S., S. Lovejoy, D. Schertzer, 2004: Multifractal surfaces and topography, *Euro Phys. Lett.*, (in press).

Gupta, V.K., and Waymire, E.C., 1997: Reply, *J. Appl. Meteor.*, **36**, 1304-1304.

Iacobellis, S., and R.C.J. Somerville, 1991a: Diagnostic modeling of the Indian monsoon onset. Part I: Model description and validation., *J. Atmos. Sci.*, **48**, 1948-1959.

Iacobellis, S., and R.C.J. Somerville, 1991b: Diagnostic modeling of the Indian monsoon onset. Part II: Budget and sensitivity studies., *J. Atmos. Sci.*, **48**, 1960-1971.

Lazarev, A., D. Schertzer, S. Lovejoy, and Y. Chigirinskaya, 1994: Unified multifractal atmospheric dynamics tested in the tropics: part II, vertical scaling and Generalized Scale Invariance, *Nonlinear Processes in Geophysics*, **1**, 115-123.

Lilley, M., S. Lovejoy, K. Strawbridge, and D. Schertzer, 2004: 23/9 dimensional anisotropic scaling of passive admixtures using lidar aerosol data, *Phys. Rev. E*, (in press).

Lovejoy, S., P. Gabriel, A. Davis, D. Schertzer, and G.L. Austin, 1990: Discrete Angle Radiative Transfer. Part I: scaling and similarity, universality and diffusion, *J. Geophys. Res.*, **95**, 11699-11715.
Lovejoy, S., and D. Schertzer, 1990: Multifractals, Universality classes and satellite and radar measurements of cloud and rain fields, *J. Geophys. Res.*, **95**, 2021.

Lovejoy, S., and D. Schertzer, 1991: Multifractal analysis techniques and the rain and clouds fields from 10-3 to 106 m, in *Non-linear variability in geophysics: Scaling and Fractals*, 111-144, Kluwer.

Lovejoy, S., and D. Schertzer, 1995: How bright is the coast of Brittany? Fractals in Geoscience and Remote Sensing, *Image understanding research series* , **1**, 102-151.

Lovejoy, S., Schertzer, D., and J.D. Stanway, 2001: Direct Evidence of planetary scale atmospheric cascade dynamics, *Phys. Rev. Lett.*, **86** (22), 5200-5203.

Lovejoy, S., D. Schertzer, and A.F. Tuck, 2004: Fractal aircraft trajectories and non-classical turbulent exponents, *Phys. Rev. E*, (in press).

Mandelbrot, B.B., and J.W. Van Ness, 1968: Fractional Brownian motions, fractional noises and applications, *SIAM Review*, **10**, 422-450.

Monin, A.S., 1972: Weather forecasting as a problem in physics, MIT press, Boston, Massachusetts.

Pedlosky, J., 1979: Geophysical fluid Dynamics, Springer-Verlag, Berlin, Heidelberg, New-York.

Ricard, J.L. and J.-F. Royer, 1993: A statistical cloud scheme for use in an AGCM, *Ann. Geophys.*, **11**, 1095-1115.

Sachs, D., S. Lovejoy, and D. Schertzer, 2002: The multifractal scaling of cloud radiances from 1 m to 1 km, Fractals, 10, 253-265.

Schertzer, D., and S. Lovejoy, 1983: On the dimension of atmospheric motions, in IUTAM Symp. on turbulence and chaotic phenomena in fluids, 141-144, Kyoto, Japan.

Schertzer, D., and S. Lovejoy, 1985a: The dimension and intermittency of atmospheric dynamics, in Turbulent Shear Flow 4, 7-33, Springer-Verlag.

Schertzer, D., and S. Lovejoy, 1985b: Generalized scale invariance in turbulent phenomena, *Physicochem Hydrodyn.*, **6**, 623-635, 1985b.

Schertzer, D., and S. Lovejoy, 1987: Physical modeling and Analysis of Rain and Clouds by Anisotropic Scaling of Multiplicative Processes, *J. Geophys. Res.*, **92**, 9693-9714.

Schertzer, D., and S. Lovejoy, 1997: Universal Multifractals do Exist!, *J. Appl. Meteor.*, **36**, 1296-1303.
Schertzer, D, S. Lovejoy, and F. Schmitt, 1995: Structures in turbulence and multifractal universality, in Small-Scale Structures in Three-Dimensional Hydrodynamic and Magnetohydrodynamic Turbulence, Proceedings of a Workshop Held at Nice, France, January 10-13, 1995 (Lecture Notes in Physics Vol. 462), Springer (New York), pp. 137-144.

Schertzer, D., S. Lovejoy, F. Schmitt, C. Naud, D. Marsan, Y. Chigirinskaya, and C. Marguerit, 1997a: New developments and old questions in multifractal cloud modeling, satellite retrievals and anomalous absorption, *Proceedings of the 7th Atmospheric Radiation Measurement Meeting,* pp. 327-335, San Antonio, Texas.

Schertzer, D., S. Lovejoy, F. Schmitt, Y. Chigirinskaya, and D. Marsan, 1997b: Multifractal cascade dynamics and turbulent intermittency, *Fractals*, **5**, 427-471.

She, Z.S., and E. Levesque, 1994: Universal scaling laws in fully developed turbulence, *Phys. Rev. Lett.*, **72**, 336.

Sommeria, G. and J.W. Deardorff, 1977: Subgrid-scale condensation in models of non-precipitating clouds, *J. Atmos. Sci.*, **34**, 344-355.

Tessier, Y., S. Lovejoy, and D. Schertzer, 1993: Universal Multifractals: theory and observations for rain and clouds, *J. App. Meteor.*, **32** (2), 223-250.